JACS
JOURNAL OF THE AMERICAN CHEMICAL SOCIETY
Communication
pubs.acs.org/JACS

Tuning the Thermoelectric Properties of Conducting Polymers in an Electrochemical Transistor

Olga Bubnova, Magnus Berggren, and Xavier Crispin*

Department of Science and Technology, Linköping University, SE-601 74 Norrköping, Sweden

Supporting Information

ABSTRACT: While organic field-effect transistors allow the investigation of interfacial charge transport at the semiconductor−dielectric interface, an electrochemical transistor truly modifies the oxidation level and conductivity throughout the bulk of an organic semiconductor. In this work, the thermoelectric properties of the bulk of the conducting polymer poly(3,4-ethylenedioxythiophene)−poly(styrene sulfonate) were controlled electrically by varying the gate voltage. In light of the growing interest in conducting polymers as thermoelectric generators, this method provides an easy tool to study the physics behind the thermoelectric properties and to optimize polymer thermoelectrics.

In the search for new thermoelectric materials, researchers estimate the potential of a material for thermoelectricity by measuring the thermoelectric figure of merit, $ZT = \sigma S^2 T/\lambda$, where T is the temperature, σ and λ are the electrical and thermal conductivities, respectively, and S is the Seebeck coefficient or thermopower.[1] To optimize ZT, the three parameters σ, λ, and S must be fine-tuned simultaneously. The Seebeck coefficient is a fundamental property of solids that characterizes the interplay between the entropy (heat) flux and the electrical current.[2] Organic conducting polymers display interesting thermoelectric properties.[3,4] Recently, the oxidation level of poly(3,4-ethylenedioxythiophene) tosylate (PEDOT-Tos) was optimized to reach ZT values as high as 0.25 at room temperature.[5] A unique feature of conducting polymers is their intrinsically low thermal conductivity, which typically ranges from 0.1 to 0.6 W m^{-1} K^{-1}.[6] Such low λ values can be reached with inorganic semiconductors only via complex strategies.[7] One approach to control S and σ of conducting polymers is controlling the redox state, for instance via chemical doping.[8] The drawback of this method is the difficulty of precisely controlling the actual doping process. Moreover, the measurement of the exact oxidation level is not straightforward, and the choice of counterions is limited.[9] Electrochemistry (electrochemical doping) typically allows better control of the oxidation level via tuning of the electrode potential and measurement of the charging current. Additionally, a large variety of counterions to balance the doping charges along the polymer chains are available simply by considering different salts in the electrolyte.

In this work, we used an organic electrochemical transistor (OECT) both to control the oxidation level of the conducting polymer and to measure its thermoelectrical properties in situ. The advantage of an OECT versus an organic field-effect transistor (OFET)[10] is that the actual electronic transport occurs within the bulk of the OECT and not only along an interface, as is the case for OFETs. Thus, an OECT can probe the actual bulk thermoelectric properties of an electrochemically active material.

In the chosen architecture, the channel and the gate were formed from the same conducting polymer and connected via an electrolyte (Figure 1b)[11,12] Poly(3,4-ethylenedioxythiophene)−poly(styrene sulfonate) (PEDOT−PSS) (Figure 1a), obtained from H. C. Starck GmbH (Clevios), functioned as the electrochemically active conducting polymer in this three-terminal OECT. The fabrication of the OECT began with patterning of Au source and drain electrodes (50 nm thick) by evaporation through a mask on a silicon substrate. PEDOT−PSS was then patterned using inkjet printing (Dimatix DMP-2800) to form a continuous film for the channel and the gate. The drop spacing was set to 25 μm, and the printer plate was kept at room temperature. The thickness of the PEDOT−PSS film was ∼50 nm as measured by a profilometer. The conducting polymer film was then annealed at 60 °C for 5 min. The active area of the channel was approximately 300 μm × 300 μm, and the size of the gate was 10 times larger to ensure full switching of the channel. A 10 wt % aqueous solution of poly(4-styrenesulfonic acid) was printed over the PEDOT−PSS channel and gate to serve as the proton-conductive electrolyte.

When there is no electric potential difference between the gate and source, the channel is in its pristine highly conducting state, and the drain current (I_D) is high as a drain−source voltage (V_{DS} in Figure 1) is applied. Once a positive gate voltage (V_G) is applied, the gate and channel are gradually oxidized and reduced, respectively, resulting in a decrease in I_D. A more detailed description of the OECT operating mechanism can be found elsewhere.[13] The two electrochemical half-reactions, one at the channel and the other at the gate, are

$$PEDOT^+PSS^- + M^+ + e^- \rightleftarrows PEDOT^0 + M^+PSS^-$$

The output characteristics are shown in Figure 1c. In the linear regime, the oxidation level in the channel is homogeneous, allowing the evolution of the thermoelectric properties of the PEDOT−PSS channel versus V_G to be correlated to specific oxidation levels. Because of its excellent chemical stability, PEDOT−PSS can undergo reversible electrochemical switching many times without degradation.

Received: May 29, 2012
Published: September 27, 2012

   dx.doi.org/10.1021/ja305188r | J. Am. Chem. Soc. 2012, 134, 16456−16459

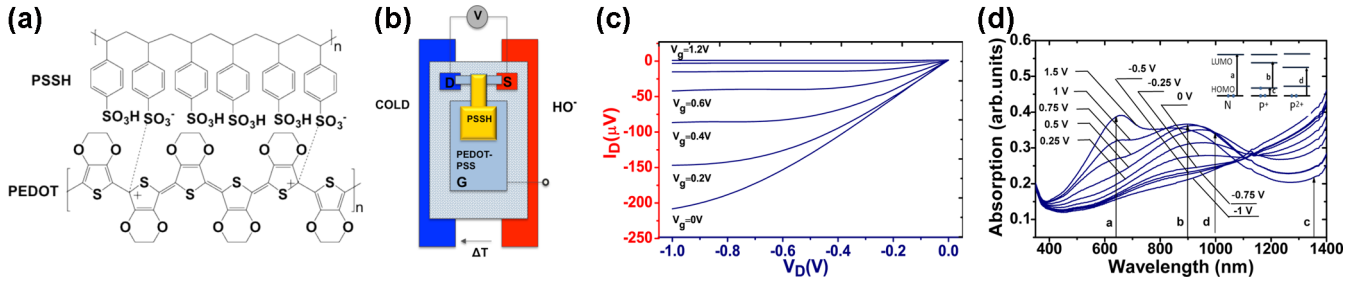

Figure 1. (a) Chemical structure of PEDOT−PSS. (b) Schematic view of the setup for thermoelectric characterization of PEDOT−PSS between the source (S) and drain (D) in a three-terminal OECT. (c) Output characteristics of the transistor. (d) In situ absorption spectra of PEDOT−PSS at various applied gate voltages V_G.

However, to investigate the properties of PEDOT in its neutral state, which is known to undergo spontaneous oxidation in air, all of the measurements were conducted under a nitrogen atmosphere. The relative humidity (RH) was kept at 60% to prevent the PSSH gel electrolyte from drying out. PEDOT−PSS displays electrochromism, and its oxidation level can thus be characterized using optical absorption spectroscopy. Depending on the applied voltage, the PEDOT−PSS channel absorbs in the visible and/or in the near-IR (NIR)[14] (Figure 1d). To characterize the Seebeck coefficient, the source and drain electrodes were placed above two metal blocks at different temperatures and separated by 2 cm, establishing a temperature difference (ΔT) of ∼2 K between the source and drain contacts. The local temperature at the transistor electrodes was read using two thermally evaporated gold thermistors (200 μm × 2 cm) separated by a distance equal to the channel's length. The thermistors were patterned on the same substrate as the OECT. Calibration of the thermistor was performed in the climate chamber to provide a resistance-versus-temperature curve.

Once the temperature difference of 2 K had been established, a specific V_G was applied for 100 s while the source and drain were kept at the same potential (ground). The gate was then disconnected (floating gate), and the electrical conductivity in the channel was measured using a standard four-point-probe method. Afterward, the thermoinduced voltage between the source and the drain (ΔV) was recorded. The Seebeck coefficient was then calculated as $S_{PEDOT} = \Delta V/\Delta T - S_{Au}$, with $S_{Au} = +1.94$ μV/K.[15] The measurements were repeated for various V_G, and the results are shown in Figure 2a as plots of electrical conductivity and Seebeck coefficient versus V_G. At negative V_G, the PEDOT−PSS channel was slightly more oxidized than in its pristine state. The electrical conductivity was 224 S/cm at $V_G = 0$ V and increased to 265 S/cm at $V_G = -0.5$ V. The Seebeck coefficient decreased from 9 μV/K at $V_G = 0$ V down to a negative value of −0.9 μV/K at $V_G = -0.5$ V. The transition from positive to negative S occurred at $V_G = -0.4$ V. The reading of the negative Seebeck coefficient was reproducible and stable over time [Figure S4a in the Supporting Information (SI)]. From −0.2 to 0.6 V, the thermopower increased quasi-linearly with V_G while the conductivity decreased exponentially. For $V_G > 0.6$ V, the Seebeck coefficient followed exponential growth while the electrical conductivity continued to decrease. The thermopower reached ∼0.4 mV/K at 1.4 V, where the conductivity was ∼0.3 S/cm. At V_G up to 2 V, S reached several mV/K, which is 3 orders of magnitude higher than the value for PEDOT in its pristine oxidized form. However, the voltage reading was too unstable for exact values to be determined. At $V_G = 2$ V, the

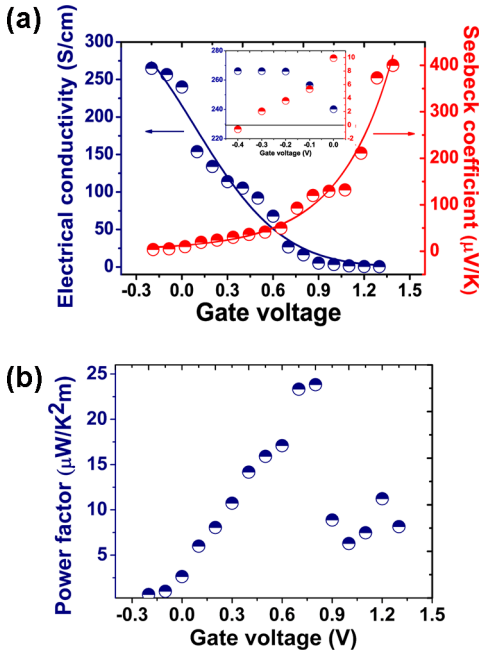

Figure 2. (a) Electrical conductivity (blue symbols) and Seebeck coefficient (red symbols) and (b) calculated power factor as functions of gate voltage.

electrical conductivity was almost 5 orders of magnitude smaller than at $V_G = 0$ V.

The evolution of the power factor σS^2 versus V_G is shown in Figure 2b. The power factor increased from 2.3 to 23.5 μW K^{-2} m^{-1} as V_G was switched from 0 to 0.8 V (corresponding to an oxidation level of 14.5%). If it is assumed that the thermal conductivity of PEDOT−PSS is independent of the oxidation level (V_G), as has been shown for polyaniline,[16] the dimensionless thermoelectric figure of merit ZT can be estimated at room temperature using the literature value λ = 0.17 W m^{-1} K^{-1}.[17] The maximum thermoelectric efficiency was obtained at an oxidation level of 14.5%, where $ZT = 0.041$ at room temperature. The oxidation level was measured at each V_G by chronocoulometry[18,19] (Figure S2). A detailed description of this method is available in the SI.

We now turn to the interpretation of the results. The electrical conductivity measured over the temperature range 295−400 K is suggestive of charge transport via phonon-assisted hopping between localized states (Figure S3)[20] with an activation energy of 0.003 eV for pristine PEDOT−PSS. Since the oxidation level of the pristine polymer was estimated at 33%, we can safely assume that for all of the oxidation levels

dx.doi.org/10.1021/ja305188r | J. Am. Chem. Soc. 2012, 134, 16456−16459

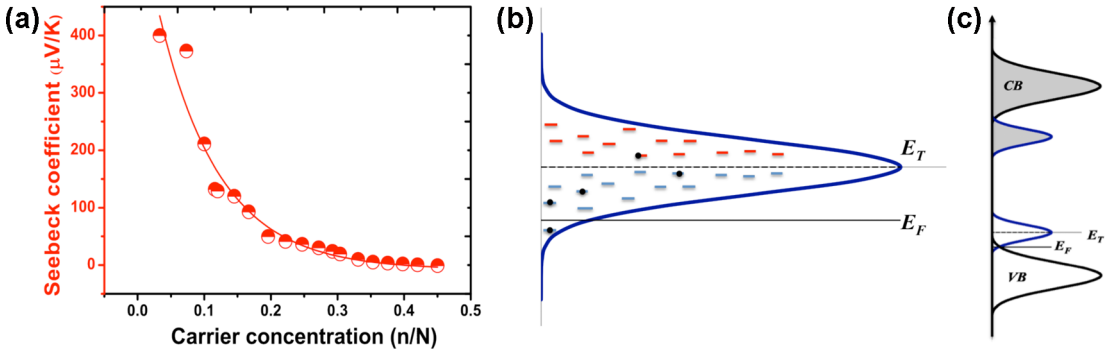

Figure 3. (a) Seebeck coefficient of electrochemically doped PEDOT−PSS as a function of fractional charge carrier concentration. The experimental results suggest exponential growth of the Seebeck coefficient upon polymer electrochemical reduction. (b) Gaussian DOS with localized states below E_T. (c) Conduction band (CB) and valence band (VB) with localized bands formed by polarons/bipolarons at the forbidden energy gap.

below this value the charge transport is likewise thermally activated. The evolution of the Seebeck coefficient and the electrical conductivity can be explained in terms of the density of states (DOS) and the probability distribution of the charge carriers in a system of interest.[21] For organic materials, the localized electronic levels involved in the transport can be characterized by a certain energy disorder represented by a Gaussian DOS of width w (Figure 3b).[22] The value of E_T, the transport energy level to which the localized charge can be promoted in a hopping process, is assumed to be fixed at the center of the Gaussian peak,[23] while doping (i.e., adding charge carriers in such a DOS) shifts the position of the Fermi level (E_F) according to the expression[24]

$$E_F = -\frac{1}{2}\left(\frac{\sigma(E)^2}{k_B T}\right) - k_B T \ln\left(\frac{1}{c}\right) \quad (1)$$

where k_B is the Boltzmann constant and $c = n/N$ is a direct estimate of the oxidation level in the conducting polymer, which contains N localized states and n charge carriers. In hopping transport, the Seebeck coefficient is proportional to $E_T - E_F$.[25] As a consequence of eq 1, the Seebeck is expected to decrease exponentially with c, in fairly good agreement with our experimental results (Figure 3a). Since the Gaussian distribution is symmetric around E_T, the Seebeck coefficient is expected to vanish at $c = 0.5$, where the Gaussian is half-filled and E_F is equal to E_T. A change in the sign of the thermopower is then only plausible at very high doping levels (i.e., above 50%). According to our experimental results, the Seebeck coefficient changes sign at a doping level of ∼46%. Note that such high oxidation levels or charge carrier densities (one of every two monomer units carries a charge) are achievable only in an OECT and not in an OFET because of the presence of screening counterions.

The main shortcoming of this model is that it does not account for a relaxation of the structure of the molecular site that carries a charge carrier. In other words, the polaronic effect is not taken into account. In conducting polymers, the existence of polarons/bipolarons [i.e., excess charge(s) localized on a structural defect on the polymer chain] is a well-established fact,[26] as indicated by vibrational and optical spectroscopies[27] and electron spin resonance spectroscopy.[28] However, the exact shape of the DOS in its disordered doped phase remains poorly understood. In PEDOT−PSS, one of the manifestations of polarons/bipolarons is the formation of the symmetric in-gap states or bands at high oxidation levels (Figure 3c), with associated electronic optical transitions in the NIR. The presence of the charged species (polarons and bipolarons) over a specific voltage range (oxidation level) is supported by the absorption spectra of PEDOT−PSS films measured at different V_G (Figure 1d). The optical transition at ∼600 nm corresponds to a neutral polymer segment (HOMO−LUMO transition; **a** in the Figure 1d inset), and the other transition at ∼900 nm is due to both polaron and bipolaron transitions (transitions **b** and **d**).[29] At negative V_G (high oxidation level), the intensities of the absorptions at 600 and 900 nm are low. This indicates that few neutral segments and few isolated polarons and bipolarons are present in the polymer films. The spectrum is characterized by a broad absorption in the IR associated with bipolaron bands (Figure 3b).[30] While a bipolaron on an isolated PEDOT chain in solution has only one main optical transition in the NIR due to symmetry,[29,31] the interaction of charged defects on the same chain creates bands whose interactions between adjacent polymer chains in the solid state creates new allowed optical transitions.[32] The broad IR absorption background is likely the result of both disordered localized bipolaronic states and the creation of intrachain and/or interchain delocalized bipolaronic bands. As V_G is increased from −1 to −0.25 V, the IR background is modified slightly. At 0 V, a peak appears at 1000 nm that is associated mostly to uncoupled bipolaron species. As the voltage increases further, the transition becomes more intense, but simultaneously, the peak shifts to 900 nm. This blue shift is attributed to an increase in polaron density (transition **b** in the Figure 1d inset) and a reduction in the amount of bipolarons (transition **d** in the Figure 1d inset). Also, the peak at 600 nm starts to increase at V_G = +0.25 V. Hence, bipolarons are transformed first into polarons, and then at higher potential, these polarons are transformed into neutral species. For V_G > 0.75 V, the polaronic peak intensity decreases whereas the peak in the visible region still increases. This suggests that the polaron concentration starts to decrease and that most of the electrochemical reaction involves the transformation of polarons into neutral segments. Hence, in the case of conducting polymers, charge carriers exist in the form of polarons or bipolarons and the transport take place in (bi)polaronic intergap bands. For a high degree of disorder, the width of the (bi)polaronic bands might be predominantly due to energy disorder rathan than energy dispersion in a (bi)polaronic band. In such a case, the localized states could be modeled with a Gaussian DOS. In these disordered systems, there is some overlap between the valence band of the neutral polymer and the polaronic/bipolaronic states, and there is always mixing

dx.doi.org/10.1021/ja305188r | J. Am. Chem. Soc. 2012, 134, 16456−16459

between the polaronic and bipolaronic states (Figure 3c). Photoelectron spectroscopy indicates the presence of those polaronic states at E_F in the DOS.[33] Further theoretical models must be developed to include those features in the quantitative estimate of the Seebeck coefficient. It should be noted that according to Mott's formula, a change in the sign of the Seebeck coefficient would correspond to a change in the derivative of the DOS, that is, S = zero when E_F is at the maximum in the shape of the DOS. Hence, such a change in sign might occur at an oxidation level that deviates to 50% for a nonsymmetrical DOS close to E_F.

In conclusion, the concept of optimizing the thermoelectric power factor of conducting polymers using electrochemical doping in an OECT has been demonstrated as a versatile tool that facilitates the control and measurement of the oxidation level. As for inorganic semiconductors, the Seebeck coefficient and the electrical conductivity are inversely dependent on the oxidation level; in other words, there is a maximum for the power factor. Because the transport occurs by phonon-assisted hopping, the evolution of the Seebeck coefficient versus the oxidation level can be qualitatively explained by assuming localized states distributed with Gaussian disorder. The Seebeck coefficient appears to change sign at oxidation levels above 50%. The exponential growth of the Seebeck coefficient with decreasing charge carrier concentration via the electrochemical reaction is related to a change in the average energy transported with the charge carriers when filling the DOS. This work has provided clear experimental evidence that further optimization of the thermoelectric properties of conducting polymers will require a better knowledge of the details of the DOS close to E_F, including the effects of disorder and the nature of the charge carriers. A priori, it would be expected that good polymer thermoelectrics might be those with sharp DOS at E_F; a first strategy would be to reduce the disorder.

■ ASSOCIATED CONTENT

Supporting Information

Experimental details. This material is available free of charge via the Internet at http://pubs.acs.org.

■ AUTHOR INFORMATION

Corresponding Author

Xavier.Crispin@itn.liu.se

Notes

The authors declare no competing financial interest.

■ ACKNOWLEDGMENTS

The authors acknowledge the Swedish Foundation for Strategic Research (Nanomaterial and Scalable TE Materials), the Knut and Alice Wallenberg Foundation (Power Paper), The Swedish Energy Agency, and the Advanced Functional Materials Center at Linköping University. We thank G. Tzamalis for his input on the absorption spectra. X.C. was supported by an ERC Starting Grant.

■ REFERENCES

(1) *CRC Handbook of Thermoelectrics*; Rowe, D. M., Ed.; CRC Press: Boca Raton, FL, 1995.
(2) Goupil, C.; Seifert, W. *Entropy* **2011**, *13*, 1481.
(3) Dubey, N.; Leclerc, M. *Polym. Phys.* **2011**, *49*, 467.
(4) Zhang, B.; Sun, J.; Katz, H.; Fang, F.; Opila, R. *ACS Appl. Mater. Interfaces* **2010**, *11*, 3170.
(5) Bubnova, O.; Ullah Khan, Z.; Malti, A.; Braun, S.; Fahlman, M.; Berggren, M.; Crispin, X. *Nat. Mater.* **2011**, *10*, 429.
(6) Hu, M.; Yu, D. *Polym. Test.* **2007**, *26*, 333.
(7) Snyder, G. J.; Toberer, E. S. *Nat. Mater.* **2008**, *7*, 105.
(8) Mateeva, N.; Niculescu, H. *J. Appl. Phys.* **1998**, *83*, 3111.
(9) Heeger, A. J. *Synth. Met.* **2002**, *125*, 23.
(10) Pernstich, K. P.; Rössner, B. *Nat. Mater.* **2008**, *7*, 321.
(11) Nilsson, D.; Chen, M.; Kugler, T.; Remonen, T.; Armgarth, M.; Berggren, M. *Adv. Mater.* **2002**, *14*, 51.
(12) Hamedi, M.; Forchheimer, R.; Inganäs, O. *Nat. Mater.* **2007**, *6*, 357.
(13) Robinson, D.; Svensson, P. *J. Electrochem. Soc.* **2006**, *153*, H39.
(14) *Organic Photovoltaics: Materials, Device Physics, and Manufacturing Technologies*; Brabec, C., Dyakonov, V., Scherf, U., Eds.; Wiley-VCH: Weinheim, Germany, 2008.
(15) Kasap, S. *Thermoelectric Effects in Metals: Thermocouples*; University of Saskatchewan: Saskatoon, SK, 1997; http://www.kasap.usask.ca/samples/Thermoelectric-Seebeck.pdf.
(16) Yan, H.; Sada, N.; Toshima, N. *J. Therm. Anal. Calorim.* **2002**, *69*, 881.
(17) Jiang, F.-X.; Xu, J.-K.; Lu, B.-Y.; Xie, Y.; Huang, R.-J.; Li, L.-F. *Chin. Phys. Lett.* **2008**, *25*, 2202.
(18) Tang, H.; Zhu, L. *Synth. Met.* **2000**, *110*, 105.
(19) Schmitz, P. H. J.; Juttner, K. *Electrochim. Acta* **1999**, *44*, 1637.
(20) Jaiswal, C. S.; Menon, M. R. *J. Phys.: Condens. Matter* **2009**, *21*, 7.
(21) Germs, W. C.; Guo, K.; Janssen, R. A. J.; Kemerink, M. *Phys. Rev. Lett.* **2012**, *109*, No. 016601.
(22) Bässler, H. *Phys. Status Solidi B* **1993**, *175*, 15.
(23) Coehoorn, R.; Pasveer, W. F.; Bobbert, P. A.; Michels, M. A. J. *Phys. Rev. B* **2005**, *72*, No. 155206.
(24) Baranovskii, S. D.; Zvyagin, I. P.; Cordes, H.; Yamasaki, S.; Thomas, P. *Phys. Status Solidi B* **2002**, *230*, 281.
(25) Fritzsche, H. *Solid State Commun.* **1971**, *9*, 1813.
(26) Brédas, J. L.; Street, G. B. *Acc. Chem. Res.* **1985**, *18*, 309.
(27) Furukawa, Y. *J. Phys. Chem.* **1996**, *100*, 15644.
(28) Zykwinska, A.; Domagala, W.; Czardybon, A.; Pilawa, B.; Lapkowski, M. *Chem. Phys.* **2003**, *292*, 31.
(29) Jeuris, K. K.; Groenendaal, L.; Verheyen, H.; Louwet, F.; De Schryver, F. C. *Synth. Met.* **2004**, *132*, 289.
(30) Chung, T. C.; Kaufman, J. H.; Heeger, A. J.; Wudl, F. *Phys. Rev. B* **1984**, *30*, 702.
(31) Beljonne, D.; Cornil, J. *Adv. Funct. Mater.* **2001**, *11*, 229.
(32) Cornil, J.; Brédas, J. L. *Adv. Mater.* **1995**, *7*, 295.
(33) Greczynski, G.; Kugler, Th.; Keil, M.; Osikowicz, W.; Fahlman, M.; Salaneck, W. R. *J. Electron Spectrosc. Relat. Phenom.* **2001**, *121*, 1.